Journal of Inorganic and General Chemistry
ZAAC
Zeitschrift für anorganische und allgemeine Chemie
www.zaac.wiley-vch.de
ARTICLE

DOI: 10.1002/zaac.201500184

Structural Variability and Gas Adsorption Properties of Coordination Polymers Constructed with Aromatic Multicarboxylic and Bidentate Ligands

Qi Chen,[a] Jian Zhang,[a] Hu Zhou,[b] and Ai-Hua Yuan*[a]

Keywords: Coordination polymers; Multicarboxylic acids; Bidentate ligands; Structure elucidation; Adsorption

Abstract. The self-assembly reactions of transition metal ions and 1,3,5-benzenetricarboxylic acid (H_3btc) in the presence of auxiliary aromatic bidentate ligands 1,10-phenanthroline (1,10-phen) or 4,4′-bipyridine-*N*,*N*′-dioxide (4,4′-bpdo) have isolated four coordination polymers $[Co_{18}(btc)_{10}(H_2O)_6(OH)_6(1,10\text{-phen})_6]\cdot 14H_2O\cdot 3DMF$ (**1**) and $[M_3(btc)_2(H_2O)_4(4,4'\text{-bpdo})]\cdot 2H_2O\cdot 2DMF$ [*M* = Co (**2**), Mn (**3**), Ni (**4**)]. Single-crystal X-ray diffraction analysis revealed that the M_3 clusters in the structure of **1**–**4** are connected by hydroxyl group oxygen atoms (or oxygen atoms from 4,4′-bpdo ligands) and carboxyl groups to generate a three-dimensional framework. The network of final assemblies can be adjusted by varying the type of auxiliary ligands (1,10-phen, 4,4′-bpdo). In addition, the gas adsorption properties of **2** are also investigated.

Introduction

Coordination polymers (or metal-organic frameworks) are well known for their rich variety of architectures and potential applications.[1,2] The use of two different ligands during the synthetic process opens up more possibilities to tune the pore size and chemical functionalities independently of the final products.[3] The successful design and construction of these materials are mainly based on the concept of network design, where the configurations of ligands are critically important. In the past few years, mixed ligands of aromatic polycarboxylic acids (O-donor) and N-donor ligands have been widely used to construct porous functional coordination polymers, because of their flexible coordination modes with central metal atoms.[4–8] However, no specific structural prediction and design scheme is available at this stage, although coordination polymers based on mixed ligands have been heavily developed in the broad domain of study. Recently, the O-donor carboxylate acid 1,3,5-benzenetricarboxylate (H_3btc) and the N-donor aromatic ligands 1,10-phenanthroline (1,10-phen) or 4,4′-bipyridine-*N*,*N*′-dioxide (4,4′-bpdo) have been employed as mixed ligands by our group to react with transition metal ions in *N*,*N*′-dimethylformamide (DMF) through solvothermal methods, isolating four new three-dimensional (3D) coordination polymers $[Co_{18}(btc)_{10}(H_2O)_6(OH)_6(1,10\text{-phen})_6]\cdot 14H_2O\cdot 3DMF$ (**1**) and $[M_3(btc)_2(H_2O)_4(4,4'\text{-bpdo})]\cdot 2H_2O\cdot 2DMF$ [*M* = Co (**2**), Mn (**3**), Ni (**4**)]. In this contribution, we report the syntheses and crystal structures of **1**–**4**, together with the gas adsorption properties of **2**.

* Prof. A.-H. Yuan
E-Mail: aihuayuan@163.com
[a] School of Environmental and Chemical Engineering
Jiangsu University of Science and Technology
Zhenjiang 212003, P. R. China
[b] School of Material Science and Engineering
Jiangsu University of Science and Technology
Zhenjiang 212003, P. R. China

Results and Discussion

Single-crystal X-ray diffraction analysis revealed that **1** belongs to the hexagonal $P6_3/m$ space group (Table 1). The asymmetric unit consists of three Co^{II} atoms, one and two thirds btc ligands, one coordinated water molecule, one hydroxyl group, one 1,10-phen ligand and solvent molecules (Figure 1). The carboxylate groups of btc ligands are all deprotonated, and adopt two types of coordination modes (Scheme 1, I and II).

There are two types of coordination environments around Co^{II} atoms. Each Co1 atom is five-coordinate and surrounded by one hydroxyl group oxygen atom and four oxygen atoms from three btc ligands. The coordination arrangement of Co1 can be described as a tetragonal pyramidal $[CoO_5]$ environment, and the five-coordinate Co^{II} was rarely observed previously. The Co1–O bond lengths are in the range of 1.942(3) to 2.245(3) Å (Table 2). The Co2 atom is a distorted octahedral $[CoO_4N_2]$ sphere built by two oxygen atoms from two btc ligands, two nitrogen atoms from one phen ligand, one hydroxyl group oxygen atom, and one coordinated water molecule. The average Co2–O and Co2–N distances are 2.121 and 2.135(4) Å, respectively. The coordination environment of Co2 is found in these materials with mixed ligands of carboxylate and bipyridine (or 1,10-phen).[9,10] As shown in Figure 2 (left), the central Co1 and Co2 atoms are interconnected through hydroxyl group oxygen atom and carboxyl groups from btc ligands to generate a Co_3 cluster. Each Co_3 cluster is connected to adjacent six Co_3 clusters through carboxylic groups from btc ligands, generating hexahedral channels along the c axis

Table 1. Crystal data collection and refinement parameters for **1**–**4**.

	1	**2**	**3**	**4**
Formula	$C_{171}H_{145}Co_{18}N_{15}O_{89}$	$C_{34}H_{42}Co_3N_4O_{22}$	$C_{34}H_{42}Mn_3N_4O_{22}$	$C_{34}H_{42}Ni_3N_4O_{22}$
Formula weight	4894.76	1035.51	1023.54	1034.85
Crystal system	hexagonal	monoclinic	monoclinic	monoclinic
Space group	$P6_3/m$	$P2_1/n$	$P2_1/n$	$P2_1/n$
a /Å	23.0194(15)	12.2821(17)	12.4035(5)	12.1761(10)
b /Å	23.0194(15)	14.426(2)	14.7004(6)	14.3360(11)
c /Å	12.7354(8)	12.5733(17)	12.6916(5)	12.5552(10)
α /°	90.00	90.00	90.00	90.00
β /°	90.00	113.909(2)	114.4750(10)	113.2200(10)
γ /°	120.0000	90.00	90.00	90.00
V /Å^3	5844.3(10)	2036.6(5)	2106.20(15)	2014.1(3)
Z	1	2	2	2
ρ /g·cm^3	1.391	1.689	1.614	1.706
μ /mm^{-1}	1.325	1.300	0.975	1.482
Total, unique	49870, 4447	17274, 4558	17917, 4755	15764, 3958
Observed [$I > 2\sigma(I)$]	2460	3423	4119	2941
$F(000)$	2474	1062	1050	1068
GOF on F^2	1.085	1.081	1.029	1.052
R_1, wR_2 [$I > 2\sigma(I)$]	0.0546, 0.1471	0.0480, 0.1190	0.0321, 0.0893	0.0461, 0.1089
R_1, wR_2 (all data)	0.0660, 0.1482	0.0761, 0.1414	0.0399, 0.0948	0.0531, 0.1098

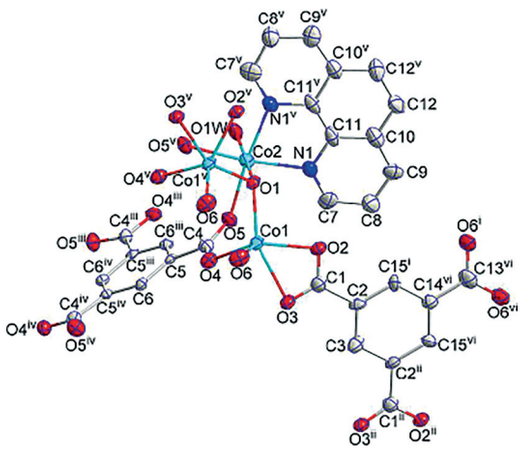

Figure 1. ORTEP diagram of **1** with displacement ellipsoids drawn at 30 % probability level. All hydrogen atoms, crystallized H_2O and DMF molecules are omitted for clarity. Symmetry codes: (i) y+1, –x+y+1, –z+1; (ii) x, y, –z+1/2; (iii) –y+1, x–y, z; (iv) –x+y +1, –x+1, z; (v) x, y, –z+3/2; (vi) 1+y, 1–x + y, z–1/2.

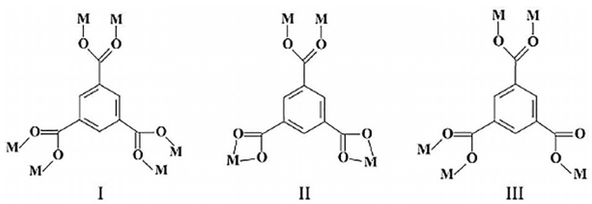

Scheme 1. Diverse coordination modes of btc ligand in the structures of **1**–**4**.

(Figure 2, right). These channels are further linked by btc ligands in the ac plane to form a 3D open framework. The uncoordinated water and DMF molecules fill the cavities and interact with the framework through hydrogen bonding interactions. The hydroxyl groups and crystallized water molecules interact with carboxyl groups from btc ligands through O–H···O hydrogen bonds. Simultaneously, the lattice water molecules are also interlinked.

When the chelated ligand 1,10-phen was replaced with the pillar ligand 4,4′-bpdo, three 3D materials **2**–**4** were isolated. Different to the chelated coordinately mode of 1,10-phen ligand in **1**, the 4,4′-bpdo ligand acts as a linker and has an obvious effect on the topology of final products. Single-crystal X-ray diffraction analysis revealed that **2**–**4** are isostructural and only the structure of **2** is descripted (Figure 3). Compound **2** crystallizes in the monoclinic $P2_1/n$ space group and the asymmetric unit includes three Co^{II} atoms, two btc ligands, four coordinated water molecules, one 4,4′-bpdo ligand, and solvent molecules. The carboxylate groups of btc ligands are all deprotonated and bridge five adjacent central Co^{II} atoms (Scheme 1, III). Co1 is an octahedral configuration coordinated by three carboxylate oxygen atoms from three btc ligands, one oxygen atom from one 4,4′-bpdo ligand and two oxygen atoms from two water molecules. The M1–O bond lengths range from 2.064(3) to 2.125(2) Å for **2** [2.1224(15) to 2.2541(15) Å and 2.014(2) to 2.092(2) Å for **3** and **4**, respectively]. The octahedral Co2 atom is occupied by four carboxylate oxygen atoms from four btc ligands and two oxygen atoms from two 4,4′-bpdo ligands. The mean M2–O bond lengths are 2.110, 2.185, and 2.083 Å for **2**, **3**, and **4**, respectively. The [CoO_6] coordination environment of Co1 and Co2 are in agreement with those found in Co-btc materials.[11,12]

As shown in Figure 4 (top), the central Co1 and Co2 atoms are linked by two btc and one 4,4′-bpdo to form a Co_3 cluster. Each Co_3 cluster is connected to adjacent ten Co_3 clusters through carboxylic groups from btc ligands, generating a 3D framework with parallelogram channels (side distances of approx. 5.8 Å × 7.2 Å) along the a axis. Then, 4,4′-bpdo ligands link adjacent Co_3 clusters and go across the channels (Figure 4, bottom). The channels were filled with crystallized water and DMF molecules, which interact with the framework of 2 through hydrogen bonds. The crystallized water molecules in-

Table 2. Selected bond lengths /Å for **1**–**4**.

1		**2**		**3**		**4**	
Co1–O1	1.998(2)	Co1–O1	2.064(3)	Mn1–O1	2.1224(13)	Ni1–O1	2.023(3)
Co1–O2	2.054(3)	Co1–O4^{iv}	2.107(3)	Mn1–O4^{iv}	2.1348(13)	Ni1–O4^{iv}	2.065(3)
Co1–O3	2.245(3)	Co1–O5	2.047(2)	Mn1–O5	2.1587(13)	Ni1–O5	2.014(2)
Co1–O4	1.984(3)	Co1–O7	2.125(2)	Mn1–O7	2.2541(13)	Ni1–O7	2.092(2)
Co1–O6	1.942(3)	Co1–O1W	2.089(3)	Mn1–O1W	2.2119(14)	Ni1–O1W	2.067(3)
Co2–N1	2.135(4)	Co1–O2W	2.103(3)	Mn1–O2W	2.1866(13)	Ni1–O2W	2.078(2)
Co2–N1^{v}	2.135(4)	Co2–O2	1.996(2)	Mn2–O2	2.0806(13)	Ni2–O2	1.984(2)
Co2–O1	2.081(4)	Co2–O2^{v}	1.996(2)	Mn2–O2^{v}	2.0806(15)	Ni2–O2^{v}	1.984(2)
Co2–O5^{v}	2.160(3)	Co2–O6	2.115(2)	Mn2–O6	2.1941(13)	Ni2–O6	2.098(2)
Co2–O5	2.160(3)	Co2–O6^{v}	2.115(2)	Mn2–O6^{v}	2.1941(13)	Ni2–O6^{v}	2.098(2)
Co2–O1W	2.081(4)	Co2–O7	2.220(2)	Mn2–O7	2.2812(12)	Ni2–O7	2.168(2)
		Co2–O7^{v}	2.220(2)	Mn2–O7^{v}	2.2812(12)	Ni2–O7^{v}	2.168(2)

Symmetry codes for **1**: (v) *x*, *y*, –*z*+3/2; for **2**: (iv) *x*–1/2, –*y*+1/2, *z*+1/2; (v) –*x*+2, –*y*+1, –*z*+1; for **3**: (iv) *x*+1/2, –*y*+3/2, *z*–1/2; (v) –*x*+1, –*y*+1, –*z*+1; for **4**: (iv) *x*+1/2, –*y*+3/2, *z*–1/2; (v) –*x*+1, –*y*+1, –*z*+1.

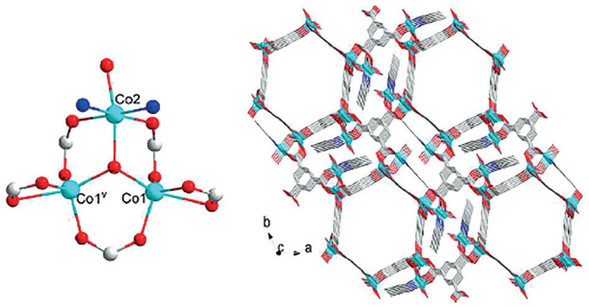

Figure 2. Co_3 cluster (left) and 3D framework (right) of **1**. Symmetry code: (v) *x*, *y*, –*z*+3/2.

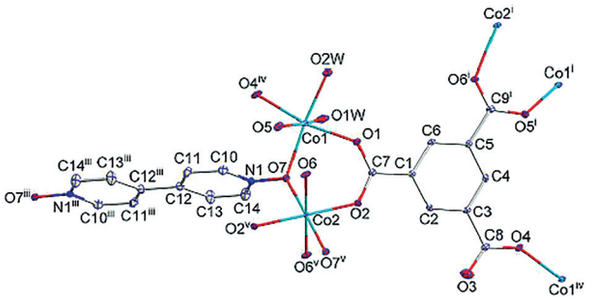

Figure 3. ORTEP diagram of **2** with displacement ellipsoids drawn at 30 % probability level. All hydrogen atoms, crystallized H_2O and DMF molecules are omitted for clarity. Symmetry codes: (i) –*x*+3/2, *y*–1/2, –*z*+1/2; (iii) –*x*+2, –*y*+1, –*z*+2; (iv) *x*–1/2, –*y*+1/2, *z*+1/2; (v) –*x*+2, –*y*+1, –*z*+1.

teract with carboxyl groups from btc ligands and lattice DMF molecules through O–H···O hydrogen bonds, whereas the lattice water molecules are interlinked by O–H···O hydrogen bonds.

Powder X-ray diffraction (XRD) patterns (Figure 5) of polycrystalline samples of **1**–**4** are in accordance with those simulated from single-crystal diffraction data, indicating high purities of products. TG curves of **1** and **2** are shown in Figure 6. For **2**, the initial weight loss (9.97 %) from 23 °C to 98 °C corresponded to the release of two guest water molecules and one DMF molecule (calcd. 10.53 %). No weight loss was observed in the range of 98–200 °C, and the framework decomposed upon further increasing temperatures. Unfortunately, **1** has a lower thermal stability than **2**, and the framework began to decompose with increasing the temperatures.

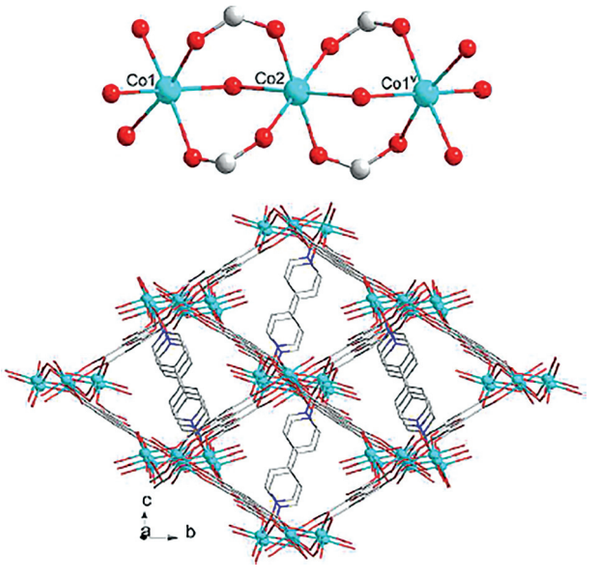

Figure 4. Co_3 cluster (top) and 3D framework (bottom) of **2**. Symmetry code: (v) –*x*+2, –*y*+1, –*z*+1.

Only the porosity of **2** was investigated due to the isostructural features of **2**–**4**. Fitting the Brunnauer-Emmet-Teller (BET) equation from the nitrogen adsorption isotherm gives the surface area of 7.2 $m^2 \cdot g^{-1}$ (Figure 7a), obviously lower than that (784 $m^2 \cdot g^{-1}$) observed in Co(Hbtc)(4,4′-bpy).[13] An additional amount at higher pressures is adsorbed, most probably multilayers on the external surface. The significantly low BET value can be reasonably attributed to the condensed structure as confirmed by single-crystal structural analysis. The hydrogen and carbon dioxide uptakes (Figure 7b) for **2** at approx. 1 atm and 77 K were 0.9 and 1.1 $mmol \cdot g^{-1}$, respectively, which are remarkably high when compared to the nitrogen adsorption capacity. The greater uptakes of H_2 and CO_2 over that of N_2 under the similar condition may be ascribed to the different kinetic diameters of gases [3.64 Å (N_2), 2.89 Å (H_2), and 3.3 Å (CO_2)].

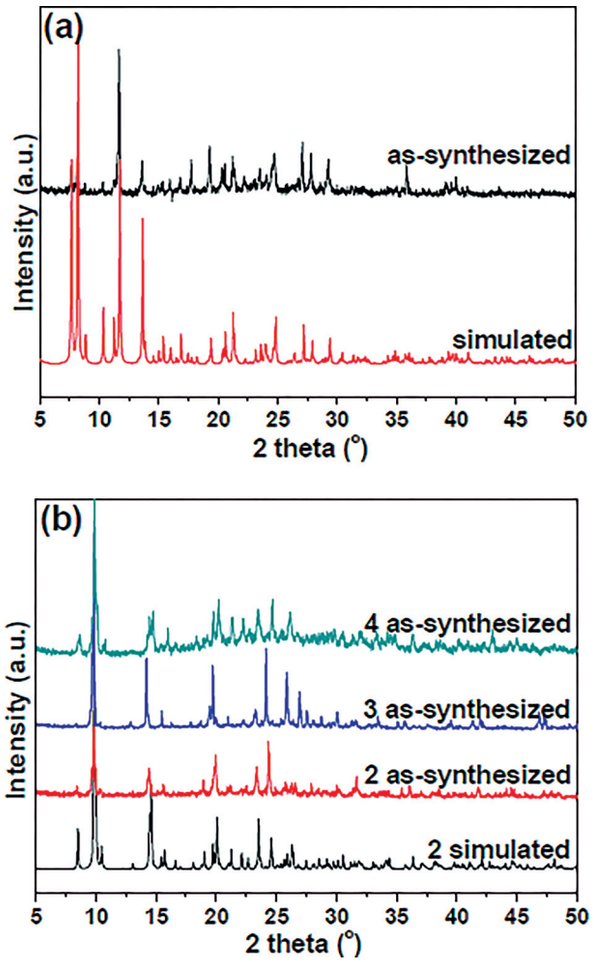

Figure 5. Powder XRD patterns of as-synthesized (a) **1** and (b) **2**–**4**, and simulated from single crystal diffraction data.

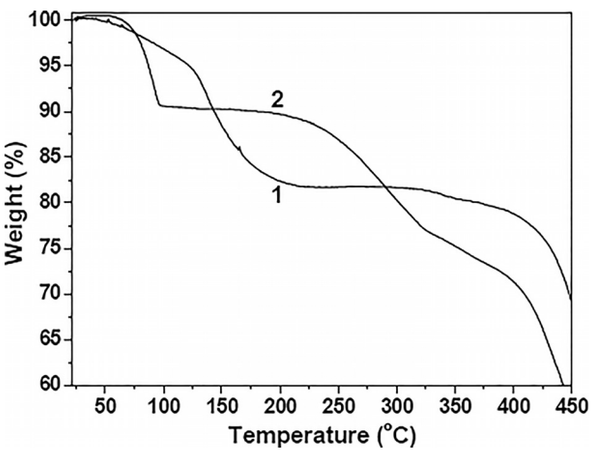

Figure 6. TG curves of **1** and **2**.

Conclusions

Four three-dimensional coordination polymers **1**–**4** were synthesized and characterized structurally. Diverse architectures of these materials are isolated by adjusting the type of auxiliary ligands (1,10-phen, 4,4′-bpdo), which indicated that the auxiliary ligands have obvious influence on the topological structures of final products. Gas adsorption experiments showed that **2** has moderate hydrogen and carbon dioxide uptakes despite of the extremely low porosity, and this material may be candidates for gas storage materials. Further studies along this line are underway.

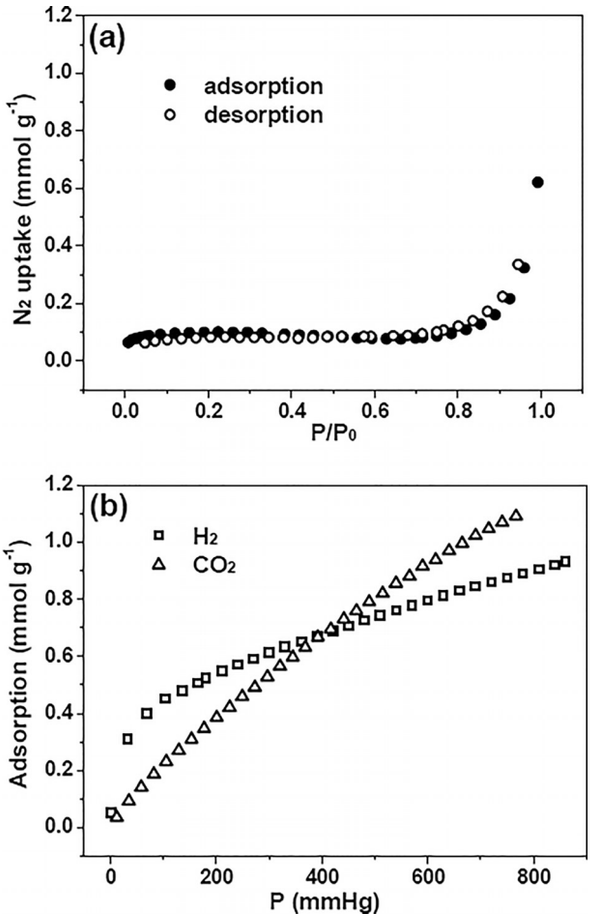

Figure 7. (a) N_2 (77 K), (b) H_2 (77 K) and CO_2 (293 K) adsorption isotherms for **2**.

Experimental Section

Materials and General Methods: All chemicals and solvents were purchased from commercial sources and used without further purification. 1,3,5-benzenetricarboxylic acid (H_3btc), 1,10-phenanthroline (1,10-phen), 4,4′-bipyridine-*N*,*N*′-dioxide (4,4′-bpdo) and *N*,*N*′-dimethylformamide (DMF) were purchased from J & K CHEMICA in a reagent grade and used without any purification. Powder X-ray diffraction patterns were collected at 4 K·min^{-1} with Cu-K_α radiation using a Shimadzu XRD-6000 diffractometer. Thermogravimetry (TG) analyses were carried out at a ramp rate of 15 K·min^{-1} in a nitrogen atmosphere with a Perkin-Elmer Pyris Diamond TGA analyzer. The gas adsorption isotherms were measured using an automatic volumetric adsorption equipment (ASAP 2020, Mircomeritics). Proceeding to gas sorption experiments, polycrystalline samples of **2** were activated at 140 °C under vacuum over 12 h. The adsorption isotherms of N_2, H_2, and CO_2 of **2** were measured at 77 K, 77 K, and 293 K, respectively.

Preparation of $[Co_{18}(btc)_{10}(H_2O)_6(OH)_6(1,10\text{-phen})_6]\cdot 14H_2O\cdot 3DMF$ (1): A mixture of $Co(NO_3)_2\cdot 6H_2O$ (0.15 mmol), H_3btc (0.15 mmol), 1,10-phen (0.15 mmol) combined with 10 mL DMF and 4 mL H_2O was stirred for 30 min. The solution was heated to 100 °C in a 20 mL Teflon-lined stainless-steel vessel, and maintained at 100 °C for 24 h, followed by slow cooling (3 $K\cdot h^{-1}$) to room temperature. Purple rod-shaped crystals were collected by filtration, washed with DMF, and dried in air. Yield: 32% (based on Co salt). $C_{171}H_{145}Co_{18}N_{15}O_{89}$: calcd. C 41.96; H 2.99; N 4.29%; found: C 41.85; H 3.05; N 4.28%.

Preparation of $[M_3(btc)_2(H_2O)_4(4,4'\text{-bpdo})]\cdot 2H_2O\cdot 2DMF$ [M = Co (2), Mn (3), Ni (4)]: A mixture of $Co(NO_3)_2\cdot 6H_2O$ (0.15 mmol), H_3btc (0.15 mmol), 4,4'-bpdo (0.15 mmol) combined with 10 mL DMF and 4 mL H_2O was stirred for 30 min. The solution was heated to 100 °C in a 20 mL Teflon-lined stainless-steel vessel, and maintained at 100 °C for 24 h, followed by slow cooling (3 $K\cdot h^{-1}$) to room temperature. Dark-red rod-shape crystals were collected by filtration, washed with DMF, and dried in air. Yield: 35% (based on M salt). Substituting $Mn(CH_3COO)_2\cdot 6H_2O$ and $NiSO_4\cdot 6H_2O$ for $Co(NO_3)_2\cdot 6H_2O$ in the synthesis procedure of **3** and **4** resulted in the formation of red rod-shaped crystals (**3**) and yellow rod crystals (**4**). Yield: 33% and 38% (based on M salt) for **3** and **4**, respectively. $C_{34}H_{42}Co_3N_4O_{22}$ (**2**): calcd. C 39.44; H 4.09; N 5.41%; found: C 39.52; H, 4.11; N, 5.35%. $C_{34}H_{42}Mn_3N_4O_{22}$ (**3**): calcd. C 39.90; H 4.14; N 5.47%; found: C 39.98; H 4.06; N 5.49%. $C_{34}H_{42}Ni_3N_4O_{22}$ (**4**): calcd. C 39.46; H 4.09; N 5.41%; found: C 39.39; H 4.13; N 5.35%.

X-ray Data Collection and Crystal Structure Renement: Diffraction data for **1**–**4** were collected with a Bruker Smart Apex II diffractometer equipped with Mo-K_α (λ = 0.71073 Å) radiation. Diffraction data analysis and reduction were performed within SMART and SAINT.[14] Correction for Lorentz, polarization, and absorption effects were performed within SADABS.[15] Structures were solved using Patterson method within SHELXS-97 and refined using SHELXL-97.[16–18] All non-hydrogen atoms were refined with anisotropic thermal parameters. The hydrogen atoms of btc, 1,10-phen, 4,4′-bpdo and DMF molecules were calculated at idealized positions and included in the refinement in a riding mode. The coordinated and uncoordinated water molecules in the structure of **1** were disordered. The hdrogen atoms bound to these water molecules were located from difference Fourier maps and refined as riding.

Crystallographic data (excluding structure factors) for the structures in this paper have been deposited with the Cambridge Crystallographic Data Centre, CCDC, 12 Union Road, Cambridge CB21EZ, UK. Copies of the data can be obtained free of charge on quoting the depository numbers CCDC-1056880 (**1**), CCDC-1056881 (**2**), CCDC-1056882 (**3**), and CCDC-1056883 (**4**) (Fax: +44-1223-336-033; E-Mail: deposit@ccdc.cam.ac.uk, http://www.ccdc.cam.ac.uk).

Acknowledgements

This research was supported by National Natural Science Foundation of China (51072072, 51272095), and Qing Lan Project of Jiangsu Province.

References

[1] J.-P. Zhang, X.-M. Chen, *Struct. Bonding (Berlin)* **2014**, *157*, 1–26.
[2] H.-C. Zhou, J.-R. Long, O.-M. Yaghi, *Chem. Rev.* **2012**, *112*, 673–674.
[3] M. Du, C.-P. Li, C.-S. Liu, S.-M. Fang, *Coord. Chem. Soc.* **2013**, *257*, 1282–1305.
[4] F.-P. Huang, J.-L. Tian, G.-J. Chen, D.-D. Li, W. Gu, X. Liu, S.-P. Yan, D.-Z. Liao, P. Cheng, *CrystEngComm* **2010**, *12*, 1269–1279.
[5] J. Seo, C. Bonneau, R. Matsuda, M. Takata, S. Kitagawa, *J. Am. Chem. Soc.* **2011**, *133*, 9005–9013.
[6] Z. Hulvey, J.-D. Fuerman, S.-A. Turner, M. Tang, A.-K. Cheetham, *Cryst. Growth Des.* **2010**, *10*, 2041–2043.
[7] J. Wang, X. Zhu, Y.-F. Cui, B.-L. Li, H.-Y. Li, *CrystEngComm* **2011**, *13*, 3342–3344.
[8] Y. Hijikata, S. Horike, M. Sugimoto, H. Sato, R. Matsuda, S. Kitagawa, *Chem. Eur. J.* **2011**, *17*, 5138–5144.
[9] L.-F. Song, C.-H. Jiang, C.-L. Jiao, J. Zhang, L.-X. Sun, F. Xu, W.-S. You, Z.-G. Wang, J.-J. Zhao, *Cryst. Growth Des.* **2010**, *10*, 5020–5023.
[10] Z.-F. Shi, L. Li, S.-Y. Niu, J. Jin, Y.-X. Chi, L. Zhang, J.-C. Liu, Y.-H. Xing, *Inorg. Chim. Acta* **2011**, *368*, 101–110.
[11] D.-P. Cheng, M.-A. Khan, R.-P. Houser, *Cryst. Growth Des.* **2004**, *4*, 599–604.
[12] M.-A. Nadeem, M. Bhadbhade, J.-A. Stride, *Dalton Trans.* **2010**, *39*, 9860–9865.
[13] Y.-Q. Li, L. Xie, Y. Liu, R. Yang, X.-G. Li, *Inorg. Chem.* **2008**, *47*, 10372–10377.
[14] Bruker; *SMART*, *SAINT* and *XPREP*, Area Detector Control and Data Integration and Reduction Software, Bruker Analytical X-ray Instruments Inc., Madison, WI, USA, **1995**.
[15] G. M. Sheldrick, *SADABS*, Empirical Absorption and Correction Software, University of Göttingen, Göttingen, Germany, **1996**.
[16] G. M. Sheldrick, *SHELXS-97*, Program for X-ray Crystal Structure Determination, Göttingen University, Göttingen, Germany, **1997**.
[17] G. M. Sheldrick, *SHELXL-97*, Program for X-ray Crystal Structure Determination; Göttingen University, Göttingen, Germany, **1997**.
[18] G. M. Sheldrick, *Acta Crystallogr., Sect. A* **2008**, *64*, 112–122.

Received: April 4, 2015
Published Online: June 16, 2015

